Eyeglasses-based Tear Biosensing System: Non-Invasive Detection of Alcohol, Vitamins and Glucose

Juliane R. Sempionatto[a], Laís Canniatti Brazaca[a,b], Laura García-Carmona[a,c], Gulcin Bolat[a], Alan S. Campbell[a], Aida Martin[a], Guangda Tang[a], Rushabh Shah[a], Rupesh K. Mishra[a], Jayoung Kim[a], Valtencir Zucolotto[b], Alberto Escarpa[c] and Joseph Wang[a]*

a. Department of NanoEngineering, University of California, San Diego, La Jolla, California 92093, United States.
b. Sao Carlos Physics Institute, University of Sao Paulo, Sao Carlos, 13566-590, Sao Paulo, Brazil.
c. Department of Analytical Chemistry, University of Alcalá, 28871 Alcalá de Henares, Spain

* Corresponding author: josephwang@eng.ucsd.edu

Supplementary Materials

Materials and Methods

Screen Printing Steps

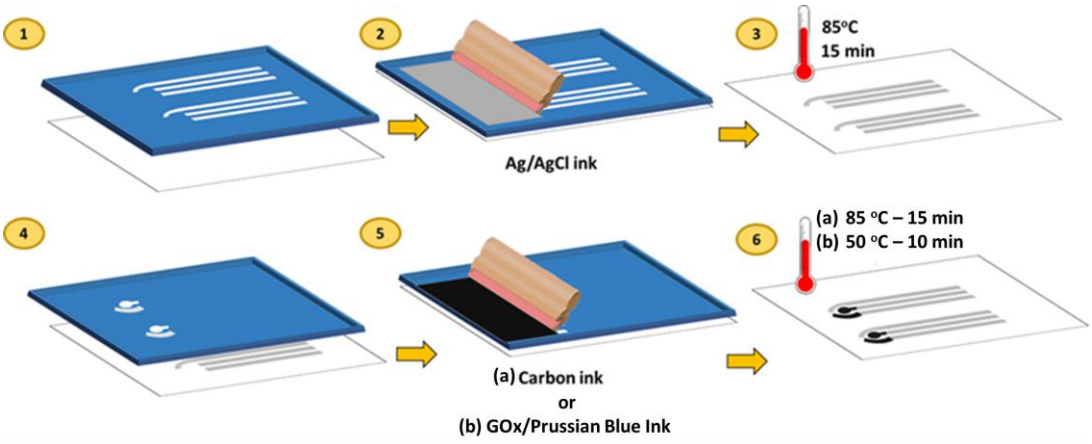

Figure S1. Screen-Printing steps for (bio)electrodes. A) Scheme showing the steps for producing screen-printed electrodes. (1) A metallic stencil with the design of the current collectors and reference electrode is placed over a PET substrate (2) Ag/AgCl ink is screen printed, using a squeegee, leaving the desired pattern on the substrate. (3) The Ag/AgCl ink is cured at 85 °C for 15 min. (4) A second metallic stencil with the working and counter electrode designs is placed over the printed silver patterns and the process is repeated. (5) Carbon ink (a) or GOx-Prussian Blue (b) ink is used to print the working and counter electrode. (6) Finally, the carbon ink is cured at 85 °C for 15 min (a) and the GOx-Prussian Blue ink is cured at 50 °C for 10 min (b).

On-body measurements with human subjects

Three healthy volunteers were asked to participate in the on-body studies. The volunteers were given the eyeglasses tear flow device fully assembled with the wireless electronic transducer. For the alcohol analysis, before every tear stimulation, the individual's blood alcohol level was checked using a commercial breathalyzer (BACtrack$^{(R)}$ s80). In the case of glucose experiments, the individual's blood glucose level was checked using a commercial glucometer (Accu-Chek Aviva Plus). A menthol tear stick (Art. #3005, Kryolan, CA, USA) was applied on the volunteer's skin at ~1 cm under the eye to stimulate a teardrop. Tear stimulation was performed as instructed in the supplier safety data sheet, which guarantees no eye damage. Skin irritation is possible after long term exposure but can be avoided with the usage of protective layers.

Tear Alcohol

The amperometric current response for the alcohol biosensor was continuously measured during all experiments. On-body alcohol monitoring experiments consisted

of two parts, before drinking and after drinking. First, with the subject being completely sober, a baseline was measured while the sensor was without any fluid. Next, the volunteer's alcohol levels were measured using the breathalyzer and tears were stimulated. Once the tear flow reached the enzyme-modified sensor through the inlet channel, the alcohol current was measured, and the signal sent to the computer via Bluetooth. The tear alcohol response was continuously measured in real-time for as long as the fluid remained inside the reservoir. The signal sharply returned to the baseline upon bringing a tissue paper into contact with the paper outlet. This procedure was repeated 2-3 times before consuming a drink to condition the biosensor, ensuring a stable signal. When the sensor reached the baseline in the last "before drinking" measurement, the subjects were asked to have a drink (~3.5 fl oz of an alcoholic beverage with alcohol content of 20 %). The "after drinking" measurement cycle was conducted as the previous step, starting 20-30 min after the alcohol consumption. The waiting period is required for alcohol to equilibrate with the bloodstream (Kim et al., 2018b, 2016). The tests were performed with the customized wireless transceiver/potentiostat mounted on the inner arm of the glasses sensor system for real-time transmission of the alcohol signals (Sempionatto et al., 2017b).

Tear Glucose

The amperometric current response for the glucose biosensor was continuously measured during all experiment. On-body glucose monitoring experiments were carried out in two parts, analogous to the tear alcohol measurements. First, a baseline was measured while the sensor was without any fluid, next, the blood glucose levels were measured, and tears were stimulated. Once the tear flow reached the enzyme-modified sensor through the inlet channel, the glucose current was measured, and the signal sent to the computer via Bluetooth. The glucose signal was continuously measured in real time for as long as the tears remained inside the reservoir. Upon removing moisture using tissue paper, the signal returned to baseline. This procedure was repeated 2-3 times before consuming a meal. When the sensor reached the baseline in the last "before meal" measurement, the subjects were asked to have a meal. A new cycle of measurements started 15 minutes after the subject completed eating. This waiting period is required for glucose to equilibrate with the bloodstream (10 min) and the tears (~5 min after the bloodstream) (Zhang et al., 2011). All tests were performed using our previous published a wireless transceiver mounted on the inner arm of the glasses sensor system for real-time transmission of the glucose signals (Sempionatto et al., 2017a, 2017b).

Tear Vitamins

On-body tear vitamin monitoring was carried out by square-wave voltammetry. Three volunteers were asked to supplement vitamin pills orally prior to each measurement. A control experiment was performed, by measuring tear vitamin, before taking any vitamin tablet. For the control experiment, tears were stimulated every 30 minutes, collected by the tears flow device and measured. The SWV was recorded only after the device's reservoir was filled with tears. After the control baselines were obtained,

vitamins (C, B_2 or B_6) were taken and the signal was recorded every 30 minutes in a similar fashion as the control. Both control and vitamin monitoring experiments were performed within 2 h.

All on-body experiments were performed in strict compliance with the guidelines of the Institutional Review Board (IRB) and were approved by the Human Research Protections Program at the University of California, San Diego (project name: Epidermal Electrochemical Sensors and Biosensors; project number: 130003).

Results and Discussion

Device Optimization

Channel dimensions and capillary pressure

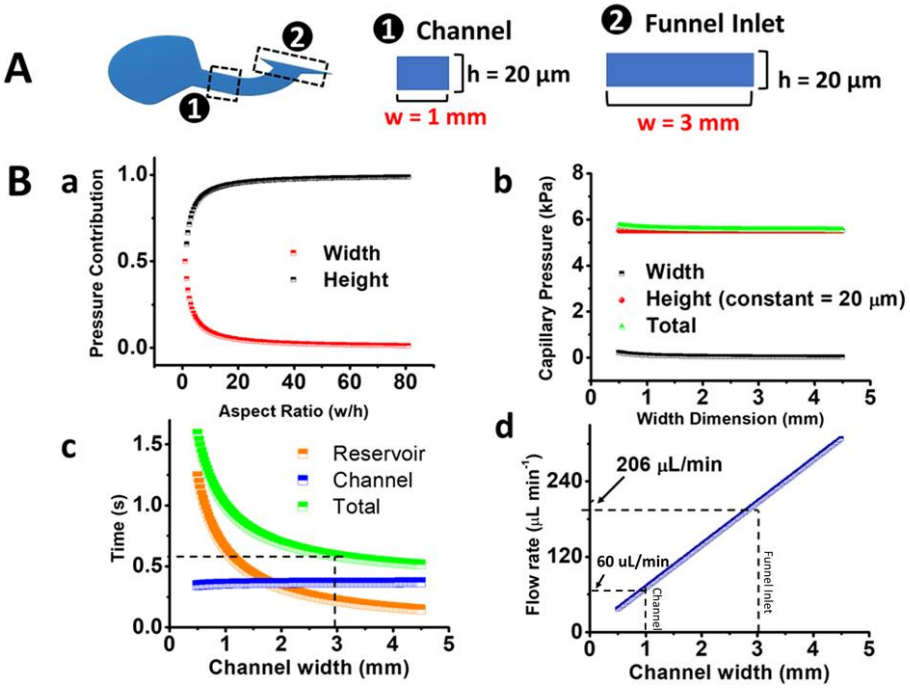

Figure S2. Channel dimensions and capillary pressure. **A)** Schematic showing the device inlet and channel dimensions. **B)** (a) Pressure contribution vs ratio of inlet width to height (w/h) where width is the black curve and height the red curve. (b) Capillary pressure dependency (green curve) with the inlet width (black curve) and constant a height of 20 µm (red curve). (c) Total time to fill the device (green curve), time to fill the reservoir (orange curve) and time to fill the channel (blue curve) when varying the channel width (w). (d) Volumetric flow rate changes with channel width.

The final goal of our wearable flow device is to collect and analyze the tears on body, while the tears are still rolling down from the eyes, and to protect the sensor from possible biofluids contamination such as sweat.

In order to perform such task, the device needs to meet the following requirements:

1. Enclose the sensor;
2. Collect enough tear fluid and deliver it to the sensor;
3. Drain the analyzed fluid for the next analysis.

To meet these requirements, the device must have the following components, which can be seen in **Figure S2A:**

Inlet: used to collect the tear from the defined region close to the eye;
Channel: conducts the fluid from the inlet to the reservoir;
Reservoir: encloses the sensor and retains the fluid to be analyzed
Outlet: drains the fluid after the analysis is performed.

The device design is also constrained by geometry and materials choices. Two important constraints are the channel length that is defined by the distance from the glasses nose pad to the eye and the spacer layer thickness.

From the requirements and constraints presented, we have a basic design, where the height is 20 µm defined by the spacer used, the channel length is 7 mm (an average found to adequately fit the anatomy of the wearer), and the reservoir has a circular shape of height 20 µm and 4 mm diameter defined by the sensor geometry. Therefore, the only dimension to be optimized for the completion of the design is the channel width.

In order to define the channel width, we have to meet the requirement that the sensor reservoir must be filled within ~2 seconds, which was found to be the average time the tears spend rolling over the inlet. To determine the time to fill the reservoir, we assume that the force driving the flow is the capillary pressure (Equation S1):

$$\Delta p=(1/w+1/h)2\sigma\cos(\theta) \qquad \text{Equation S1}$$

Equation S1 can be rewritten as:

$$\Delta p=(1/w)2\sigma\cos(\theta)+(1/h)2\sigma\cos(\theta) =\Delta p_w+\Delta p_h \qquad \text{Equation S2}$$

Equation S2 shows the contribution for the capillary pressure from the change in width and Δp_w change in height Δp_h, also defining the aspect ratio as:

$$AS=w/h \qquad \text{Equation S3}$$

We can obtain the pressure contribution from the width change and from the height change:

$$\Delta p_w/\Delta p=1/(1+AS) \qquad \text{Equation S4}$$
$$\Delta p_h/\Delta p=AS/(1+AS) \qquad \text{Equation S5}$$

The contribution for the capillary pressure is plotted on **Figure S2B-a**. We can see that for AS>~20 the pressure is approximately constant, and the dominant term is Δp_h which correspond to 95% of the total pressure for AS=20. Thus, equation S1 can be approximated to:

$$\Delta p \approx (1/h)2\sigma\cos(\theta) \qquad \text{Equation S6}$$

Since the height is constant throughout the entire device, pressure is also constant (see equation S6). For a constant pressure in a rectangular channel, we can determine the flow rate from Equation S7

$$Q \approx [(h^3\, w\Delta P)/12\mu L]\,[(1-0.630)\, h/w] \qquad \text{Equation S7}$$

Equation S6 is valid for h<w and is a good approximation: e.g. for h=w the error is 13%, while for w=2h the error is 0.2%. Combining Equations S6 and S7 gives:

$$Q \approx [(1-0.630)\, h/w]\;\; [(h^2\, w\Delta P)/6\mu L]\;\sigma\cos(\theta) \qquad \text{Equation S8}$$

We applied Equation S8 to estimate the time to fill the device. It is important to note that the reservoir cross-section width is variable since it has a circular shape. In order to simplify the calculations, we approximate the circle to a rectangular channel, where w=d and L=d. This approximation overestimates the volume, therefore overestimating the time to fill the reservoir, which ensures the actual time will be less than the theoretically computed time. The results of applying Equation S8 together with those assumptions shows the time to fill the channel, reservoir, and both **(Figure S2B-c)** as function of the width, and the flow rate as function of the rectangular channel width for h=20 µm **(Figure S2B-d)**.
Another constraint arises from the manufacturing method. It is not possible to manufacture a channel with width smaller than 1 mm using the current methodology (Cutter machine "Cricut Explore Air 2"). Hence, we used 1 mm as the minimum practical width.

Optimization of the Inlet shape

The inlet channel and opening shape were experimentally optimized. Tears were collected from a volunteer and a blue food dye was added. A smooth angled (30°) platform was used to simulate the tear path on the face curvature. A volume of 20 µL of blue tears were released from a distance of 2 cm from the inlet opening. Several channels and features were tested, the results are shown in **Table S1.**

Table S1. Inlet shape optimization. Inlet shape optimization was performed by studying the tear collection rate of 5 different designs: Regular (straight), 45° cut, C shaped, C shaped with funnel and C shaped with angle cut. Tears with blue dye were dropped from a distance of 2 cm ("X" mark) and the amount of fluid captured by the devices was assessed. The black lines indicate the limit of tears on each sensor. Only 2 of the designs were able to fill the reservoir completely: C shape and C shape with funnel, with the last one displaying the best results in repetitive tests. Therefore, the C shape with funnel (design 4) was the shape used for the final device.

Design	Features	Volume collected	Result
1. Regular	• Straight Inlet • Straight cut • Total lenght 7 mm		• Not enough tears collected • Fills up ~50% of the total volume
2. 45o cut	• Straight inlet • 45° cut • Total lenght 7 mm		• Not enough tears collected • Fills up ~80% of the total volume
3. C shaped	• C shaped inlet • Straight cut • Total lenght 7 mm		• Enough tears collected • Fills up total volume
4. C shaped with funnel	• C shaped inlet • Funnel cut • Total length 7 mm		• Excess of tears is collected • Fills up total volume
5. C shape angle cut	• C shaped inlet • 30° cut • Total lenght 7 mm		• Not enough tears collected • Fills up ~40% of the total volume

In vitro characterization of electrochemical tear alcohol biosensors

Since the alcohol biosensor will be used for the monitoring of tear alcohol in tear flow (with the flowing tears entering the device = 206 µL/min c.a.), the analytical performance of the AOx-modified PB detector was evaluated first *in vitro* using flow injection analysis (FIA) with amperometric detection, as well as in a static

environment. A flow rate similar to tear flow was used to assess the stability of the bio-recognition layer toward leaching of the biomaterials, by pumping the PBS solution at 200 µL/min. The stability of the fluidic-based biosensor was studied for 11 consecutive measurements. For this evaluation, a 10 mM ethanol solution was injected during continuous PBS flowing conditions. The biosensor flow detector displayed good reproducibility (RSD < 6.9 %, n=11) (**Figure S3A-a**), with well-defined peak currents that increased linearly upon increasing the ethanol concentration (**Figure S3A-a and S3B**) with the corresponding calibration plot displaying good linearity and sensitivity (-0.079 ± 0.004 mM/µA), linearity (R^2=0.924) and repeatability (RSD<1.8 %, n=3); see details in the supporting information. The sensor was evaluated also for potential interfering constituents of tears at higher concentrations than their expected physiological levels. The results showed negligible signals for the injections of 5 mM lactate, 1.2 µM uric acid, 8 mM urea, 8 µM ascorbic acid and 0.1 mM acetaminophen (**Figure S3A-c**). Ethanol calibration was performed also in static conditions (**Figure S3C**), displaying a sensitivity of -0.011 ± 0.001 µM/µA, with good linearity (R^2=0.964). Interference experiments, conducted also using static conditions, confirmed the high selectivity observed under flow conditions (**Figure S3D**).

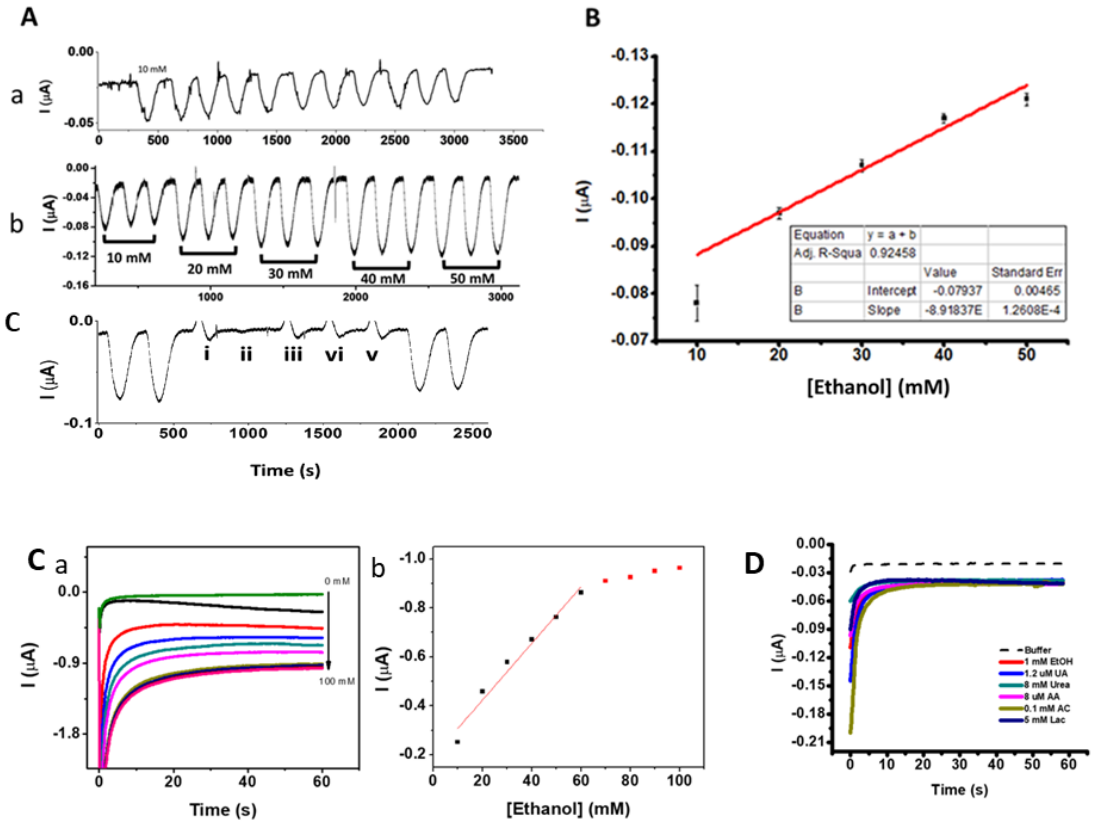

Figure S3. In-vitro characterization of electrochemical alcohol biosensors by FIA and static mode. A) (a) Stability study. Intensity current at -0.1 V for a fixed glucose concentration (10 mM) on PBS 0.1 M pH = 7.4 measured consecutively. (b) Chronoamperogram obtained at -0.1 V in PBS using flow injection pumped at 200 µL/min for ethanol concentration varying from 10 to 50 mM with 10 mM additions. (c) Amperometric flow injection interference study: response obtained at -0.1 V in PBS flowing at 200 µL/min with injections

of 40 mM ethanol followed by (i) 5 mM lactate, (ii) 1.2 µM uric acid, (iii) 8 mM urea, (iv) 8 µM ascorbic acid, (v) 0.1 mM acetaminophen, and 40 mM ethanol, respectively. B) Calibration curve obtained from the chronoamperogram obtained at -0.1 V in PBS using flow injection pumped at 200 µL/min for ethanol concentration varying from 10 to 50 mM with 10 mM additions. (C) (a) Chronoamperogram response for increasing ethanol concentration in static PBS (0-100 mM, 10 mM increment). (b) Calibration curve corresponding to the amperometric response under static conditions. (D) Static interferent test. Additions of: 0.1M PBS Buffer, 1 mM EtOH, 1.2 µM uric Acid, 8 mM urea, 8 µM ascorbic acid, 0.1 mM acetaminophen, and 5 mM lactate.

Tears alcohol detection with collected tears

To study the correlation between tears alcohol and BAC, an *in vitro* analysis was performed with tears collected from three volunteers. The monitoring of alcohol in tears was performed in two steps. The first step was simple evaluation of the tears alcohol response using the AOx-modified biosensor by monitoring tear alcohol levels before and 30 min after an alcohol intake (**Figure S4A-a**). For this experiment, tears were stimulated, collected and measured using the modified biosensor, as shown in **Figure S4A-b**. An increase in the current signal was obtained after alcohol consumption for all volunteers, with the response being proportional to concurrent BAC levels (**Figure S4B**). In the second step of the *in vitro* study, the subjects were asked to collect tears three separate times (in the same fashion as the first step), before alcohol intake, followed by 30 min and 2h after the intake (when BAC returned to ~ 0.000 %) to evaluate carry-over effects of the biosensor. In all steps, the alcohol in tears was measured as soon as the tears were collected using one single electrode for each volunteer, dried out using paper capillarity, and the electrodes were left at room temperature during all experiments. The resulting chronoamperograms showed increasing current after the alcohol intake followed by a return to baseline once the BAC reached 0.000 % (**Figure S4C**). Accordingly, the results of these two *in vitro* studies indicate that the alcohol content in tears is strongly correlated to the blood alcohol levels (BAC) with Pearson's r=0.852 when correlating the current values and BAC levels of all three volunteers (**Figure S6**). This profile demonstrates the attractive stability and absence of carry-over effects, indicating the potential of the tears alcohol biosensor for non-invasive monitoring of blood alcohol in a continuous manner, including repetitive cycling of sober and drunk states. The difference in the BAC response and in the time to reach BAC=0.000% among the individual subjects upon consuming the same amount of alcohol reflects their different alcohol metabolism rates.

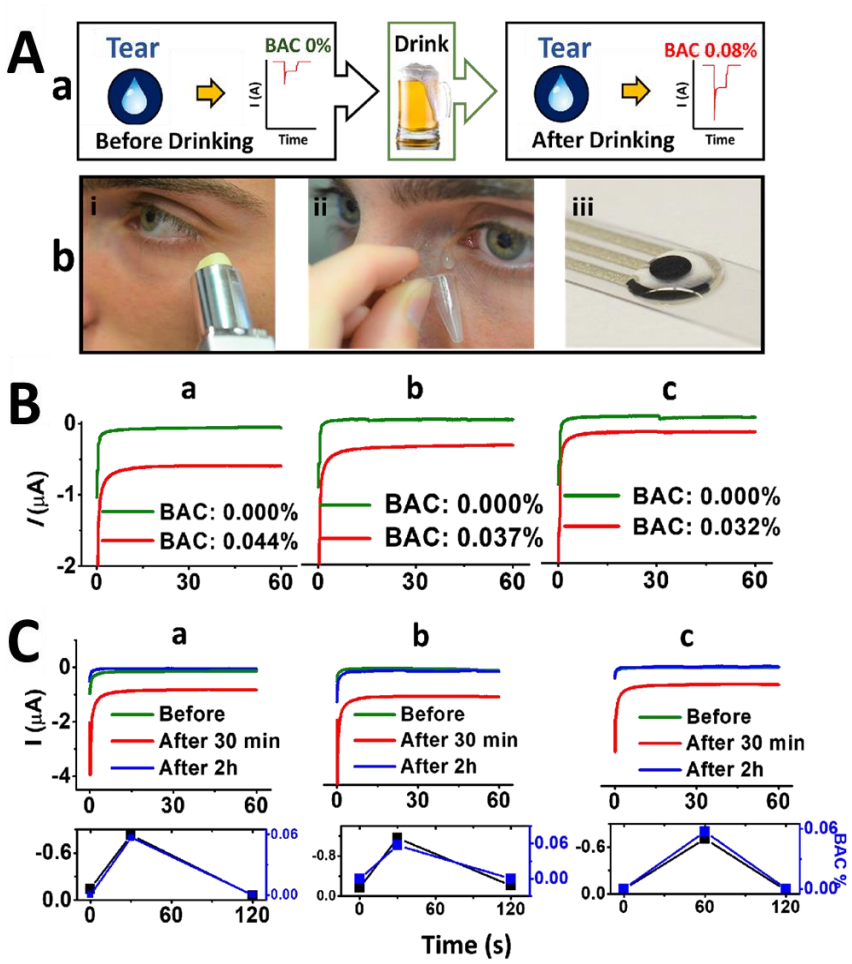

Figure S4. in-vitro characterization of the microflow-cell alcohol detector. A) *In vitro* electroanalysis of collected tears. a) Timeline used for alcohol tears detection. b) (i-ii) Tears stimulation and collection. (iii) In vitro analysis of collected tears. **B)** Chronoamperogram before drinking alcohol (green) and 30 min following the alcohol ingestion (red) for subjects a, b and c. **C)** Chronoamperograms before drinking alcohol (green), after 30 min of alcohol ingestion (red) and after 2 h of the initial drinking (blue) for subjects a, b and c.

On-body Background Testing of the Background Response

To examine signal stability, the fully integrated device was tested for tears collection, on-body monitoring without any alcohol intake using an AOx-modified biosensor. **Figure S5A** shows the continuous signal obtained after stimulating tears 8 times with 10 min intervals along with the auxiliary drying step. A stable signal was obtained after three measurements. Additionally, the sensor demonstrated a good stability with RSD < 9 % (n=8). Further, the average current response for the tears without alcohol consumption was 0.02 µA, as was observed for both on-body and *in vitro* experiments. The same current range was recorded when measuring the response of the AOx-modified electrode to 0.1M PBS. However, the current level decreased upon removing

oxygen (by purging N_2 for 20 min in the PBS solution), indicating that the residual current related solely to oxygen effects; this was supported by testing the interference of several common electroactive molecules that showed negligible current (**Figure S5B**). Various sensor coatings were evaluated to mitigate these oxygen effects, with the chitosan layer displaying the most favorable performance (**Figure S5C**).

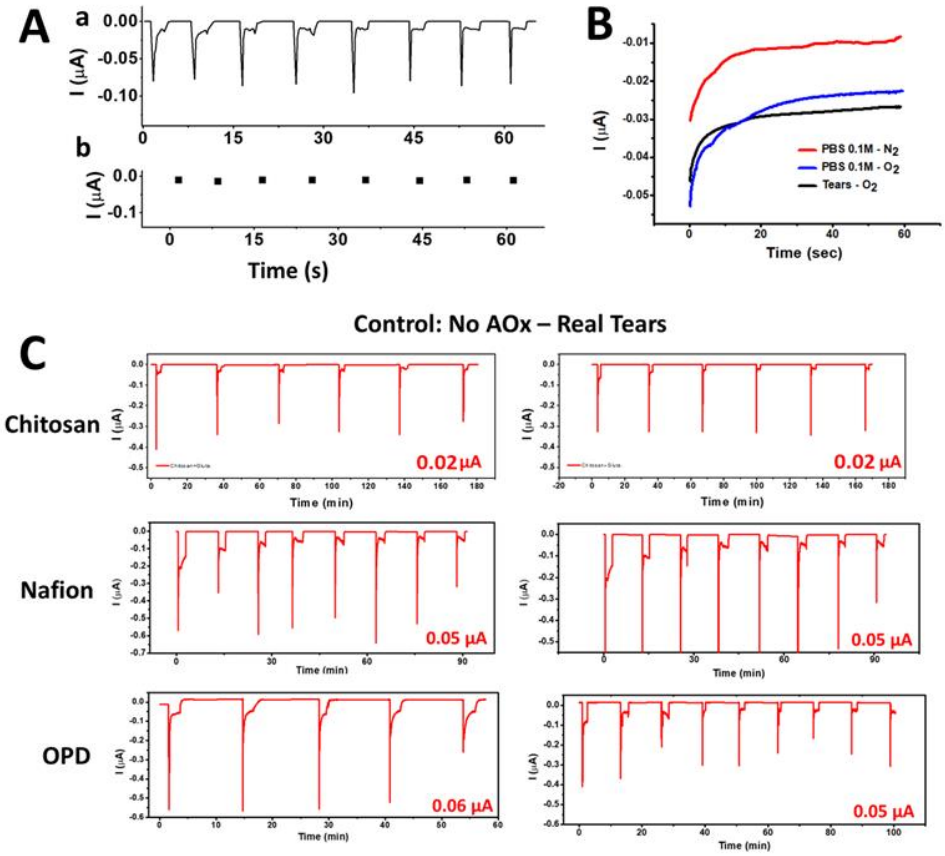

Figure S5. Testing the Background signals and Optimizing the coating layer. A) Performance of tears collection on-body test without alcohol intake. a) Tears were stimulated every 10 min and the drying step was performed after 3 min of tears collection. b) Current vs time correlation obtained from chronoamperogram in (a). **B)** Examination of oxygen effects on AOx-modified sensor response with chronoamperogram at -0.1 V under static conditions. **C)** On-body evaluation of sensor coatings for mitigation of oxygen effects on the sensor response with chronoamperogram obtained at -0.1 V.

Tears and BAC correlation curves

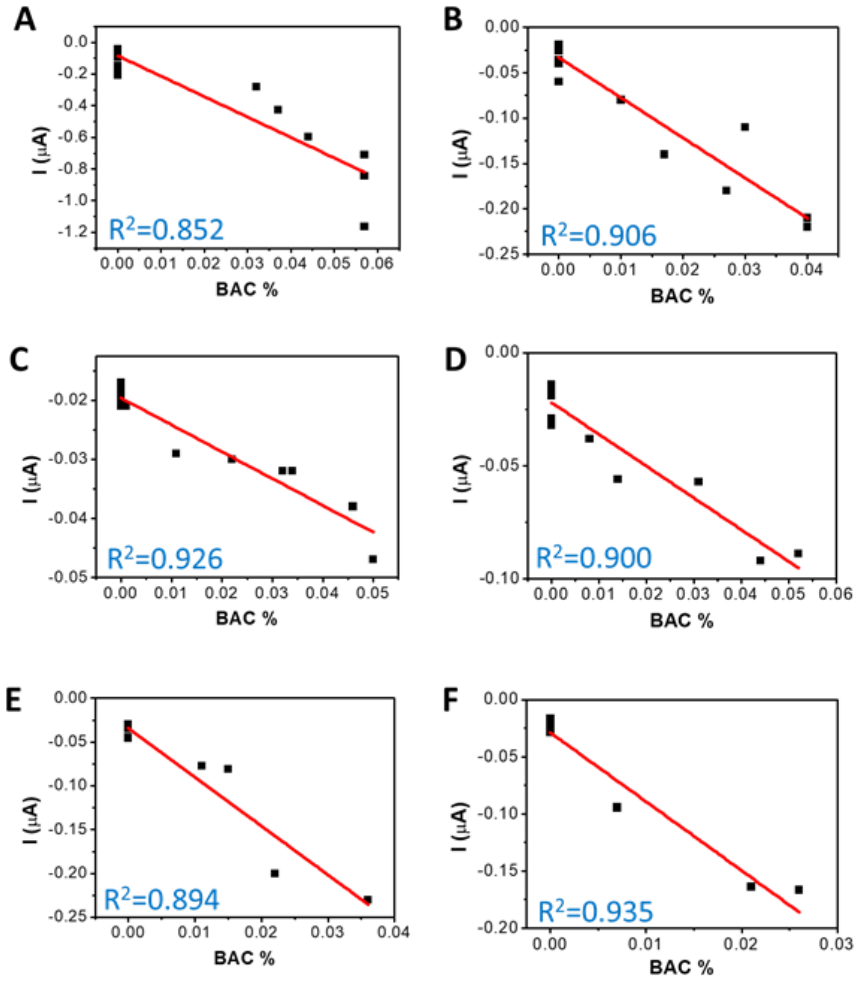

Figure S6: Correlation between blood alcohol concentration and the current measured by the microfluidic device. **A)** All *in vitro* measurements from Figure S4; **B)** Subject 1 (left) from Figure 2B; **C)** Subject 2 (middle) from Figure 2B; **D)** Subject 3 (right) from Figure 2B; **E)** Subject A from Figure 2C; **F)** Subject B from Figure 2C.

Continuous non-invasive tear glucose monitoring with human subjects using integrated eyeglasses biosensor

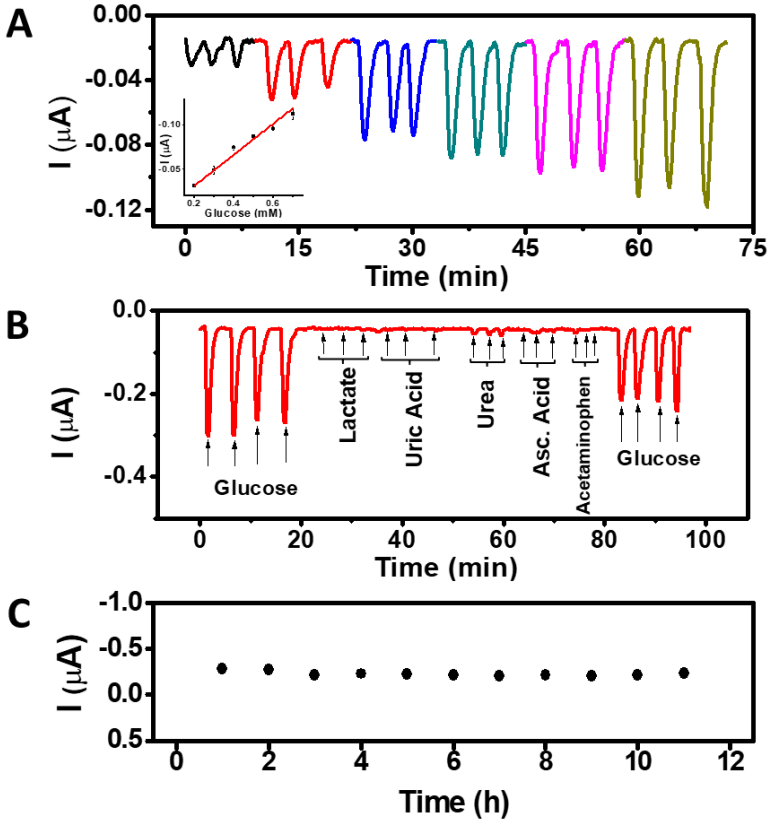

Figure S7. Glucose biosensor analytical analysis. A) Chronoamperograms obtained at -0.2 V in PBS using flow injection pumped at 200 µL/min for glucose concentration varying from 0.2 to 0.7 mM with 0.1 mM additions. (B) Chronoamperograms obtained at -0.2 V in PBS using flow injection pumped at 200 µL/min for interference test by adding 1 mM glucose, 10 mM lactate, 10 mM urea, 10 mM ascorbic acid and 1 mM glucose respectively. (C) Stability study. Current response monitored at -0.2V for a fixed glucose concentration (1 mM) on PBS 0.1M pH=7.4, measured every hour for 10 consecutive hours.

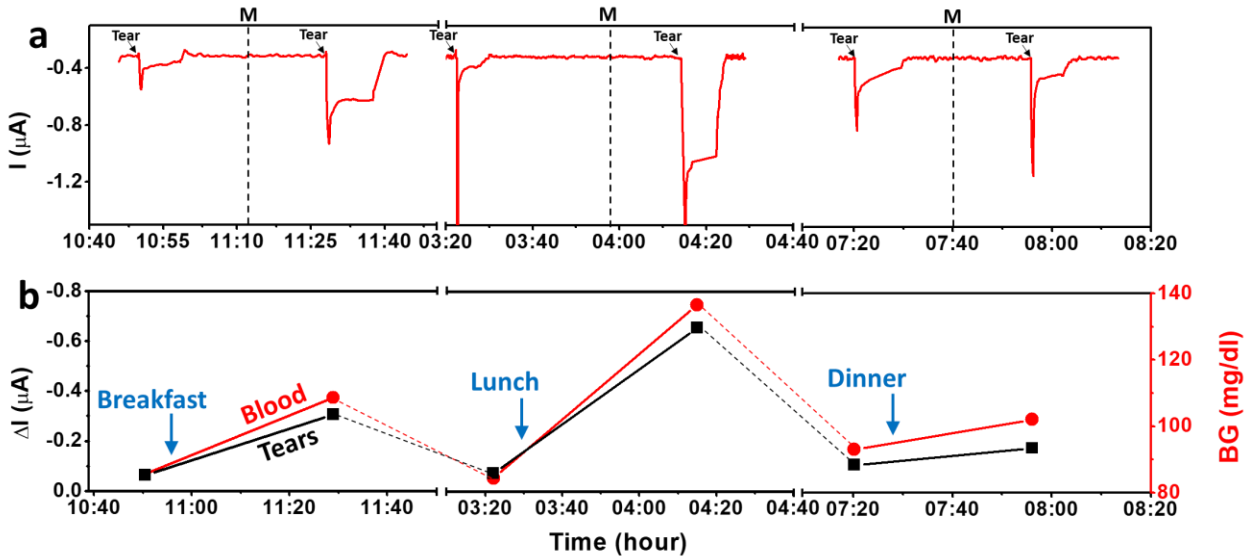

Figure S8. Whole day tear glucose monitoring. (D) Monitoring of the glucose levels during the whole day: breakfast, lunch and dinner. Pointed out: Tear stimulation and meal (M and dotted line). Bottom, correlation between glucose in blood measured with a glucometer (red) and the current intensity obtained with the wearable sensor (black).

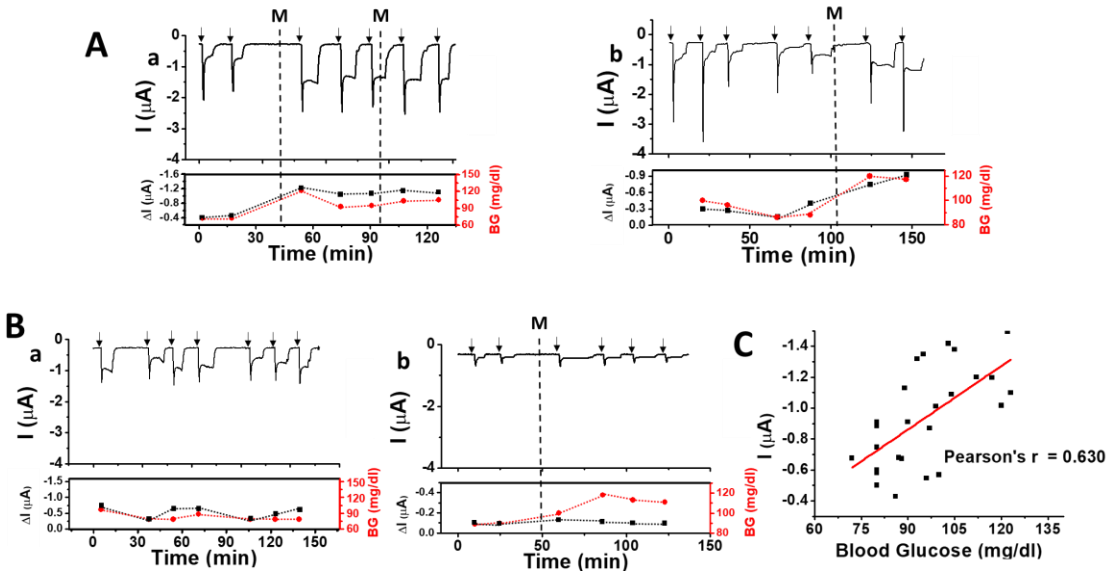

Figure S9. On body experiments performed with (Aa) two meals and (Ab) one meal. Control experiments performed with (Ba) no meal and (Bb) with one meal and no enzyme. (C) Correlation curve for blood and tear glucose, with a Pearson's correlation coefficient of 0.630.

Non-Invasive tear vitamin monitoring with human subjects using integrated eyeglasses biosensor

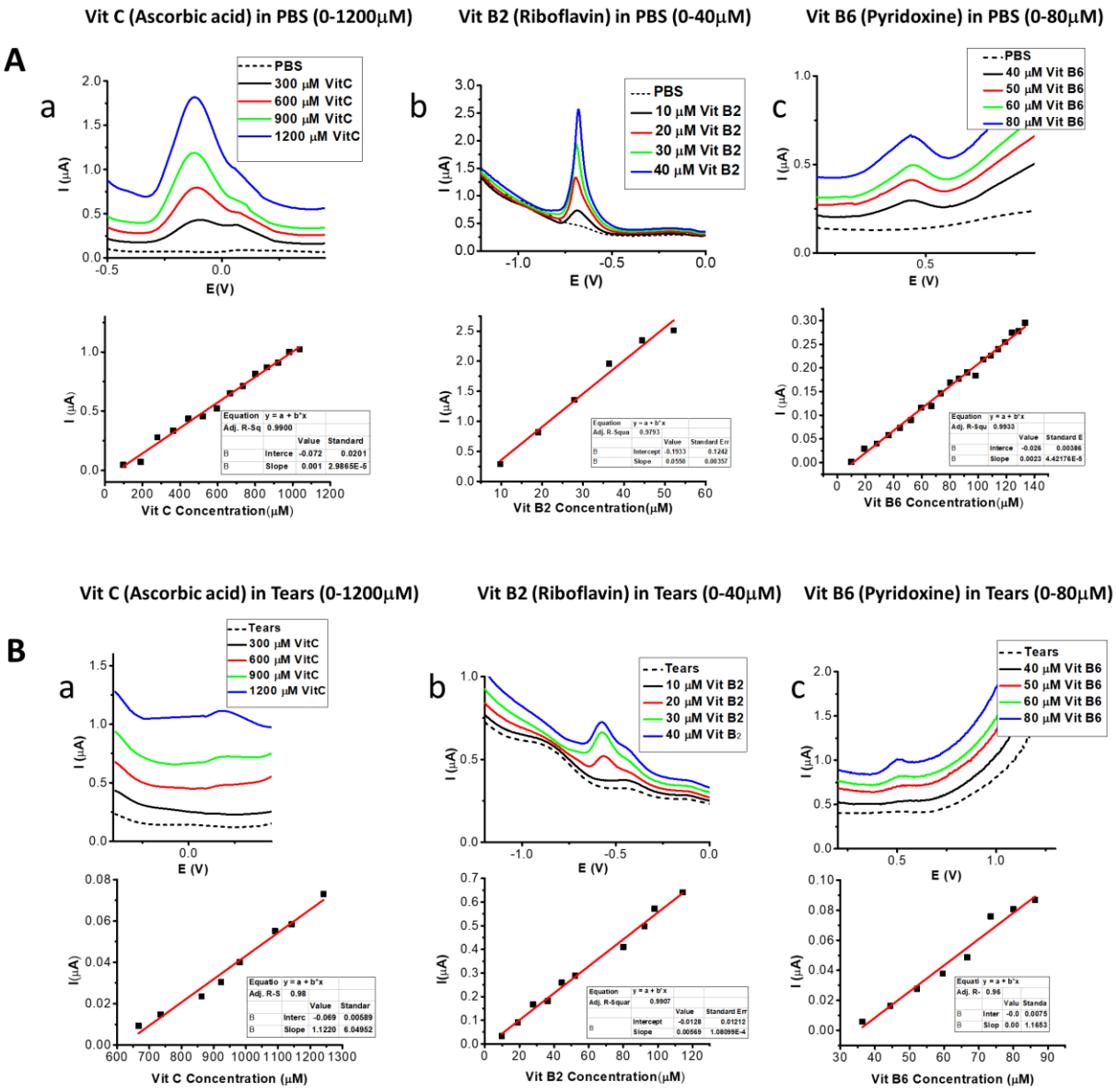

Figure S10. **PBS and tears spiked with Standard solutions of vitamins.** Square wave voltammograms of vitamins in PBS pH 7.4 and Tears spiked with different concentrations of vitamins standard solutions: A) a) vitamin B2 (10-40 mM) b) vitamin C (0.3-1.2 mM) c) vitamin B6 (40- 80 mM) in PBS and Real Tears. SWV Conditions: Potential range: -1.0 V - +1.0 V, amp: 25 mV, Freq: 10 Hz. (Potential ranges showed based on peak potentials) B) Calibration curves corresponding to vitamin concentration vs. peak currents obtained from SWVs in PBS pH 7.4 and Tears for a) vitamin B2 b) vitamin C c) vitamin B6

Support Information References

Kim, J., Sempionatto, J.R., Imani, S., Hartel, M.C., Barfidokht, A., Tang, G., Campbell, A.S., Mercier, P.P., Wang, J., 2018b. Adv. Sci. 5, 1800880.

Kim, J., Jeerapan, I., Imani, S., Cho, T.N., Bandodkar, A., Cinti, S., Mercier, P.P., Wang, J., 2016. ACS Sensors 1, 1011–1019.

Sempionatto, J.R., Nakagawa, T., Pavinatto, A., Mensah, S.T., Imani, S., Mercier, P., Wang, J., 2017b. Lab Chip 17, 1834–1842.

Sempionatto, J.R., Mishra, R.K., Martín, A., Tang, G., Nakagawa, T., Lu, X., Campbell, A.S., Lyu, K.M., Wang, J., 2017a. ACS Sensors 2, 1531–1538.

Zhang, J., Hodge, W., Hut3nick, C., Wang, X., 2011. J. Diabetes Sci. Technol. 5, 166–172.